

Full Length Research Paper

Geological and structural interpretation of the Konongo area of the Ashanti gold belt of Ghana from aeromagnetic and radiometric data

Boadi B, Wemegah D.D and *Preko K

Department of Physics, Geophysics Unit, Kwame Nkrumah University of Science and Technology, University post office, Private mail bag, Kumasi, Ghana

Abstract

Aeromagnetic and radiometric methods were used to investigate the Konongo area located at the north-eastern boundary of the prospective Ashanti Gold Belt in south-eastern Ghana. Datasets from these aerogeophysical methods proved vital for mapping geology and structure. The application of magnetic image enhancing techniques such as reduction to pole, analytical signal and first vertical derivative in processing the datasets helped in the delineation of folds, fractures, lithological boundaries and the two main Birimian tectonic structural deformation events D1 (NE-SW) / D2 (NNW-SSE) which are potential hydrothermal gold mineralization zones within the area. The contacts between Birimian meta-sedimentary and meta-volcanic rocks noted to host gold mineralization in the belt were also delineated. The radiometric datasets retrieving geochemical information on potassium (K), thorium (Th) and uranium (U) concentrations within the study area were used to delineate bedrock lithology of the Bansa Batholith, Birimian meta-volcanics, Tarkwaian formation, as well as alteration and contact zones. High K, Th and U concentrations were mapped in the meta-sediments and the Bansa batholith. The high-resolution airborne magnetic and radiometric data of the study area resulted in better definition of both geological structures and lithological boundaries. This work shows the usefulness of geophysical data in mapping possible geological structures that host hydrothermal gold mineralization within the Konongo area of the Ashanti Gold belt of Ghana.

Keywords: Aeromagnetic, aeroradiometric, hydrothermal, alteration, mineralization.

INTRODUCTION

Airborne magnetic and radiometric surveys have been used extensively in the mineral exploration industry predominantly for the delineation of metalliferous deposits (Airo and Loukola-Ruskeeniemi, 2004). Its application ranges from mineral exploration (Murphy, 2007), structure mapping and rock characterization (Telford et al., 1990). Recent advances in technology have substantially increased the accuracy and resolution of these techniques so that they can be used to provide useful enhanced information on lithology and geological structures. Additionally, advances in data analysis, processing and image enhancement techniques have improved the resolution of geophysical datasets further

so that very subtle variations in the geophysical responses can be identified (Armstrong and Rodeghiero, 2006). Geophysical techniques were used for prospecting as early as 1935 for extensive underground exploration at the Konongo mines to maintain a reserve base ahead of production. The surveys included Electrical survey carried out by the Electrical Prospecting Company of Sweden in 1935, Electromagnetics (Turam) and ground magnetic in 1967 and resistivity survey at Nanwa (extensions to Obenemase A and B lodes) in 1973.

In 1960, Hunting Surveys Limited of the United Kingdom undertook geophysical exploration for minerals in Ghana using airborne magnetic and radiometric survey with a total area coverage of 1.7×10^4 km². This included the Takoradi through Tarkwa and Prestea, Dunkwa and Obuasi to Konongo and Buem-Togo-Dahomeyan

*Corresponding Author E-mail: kpreko@yahoo.com

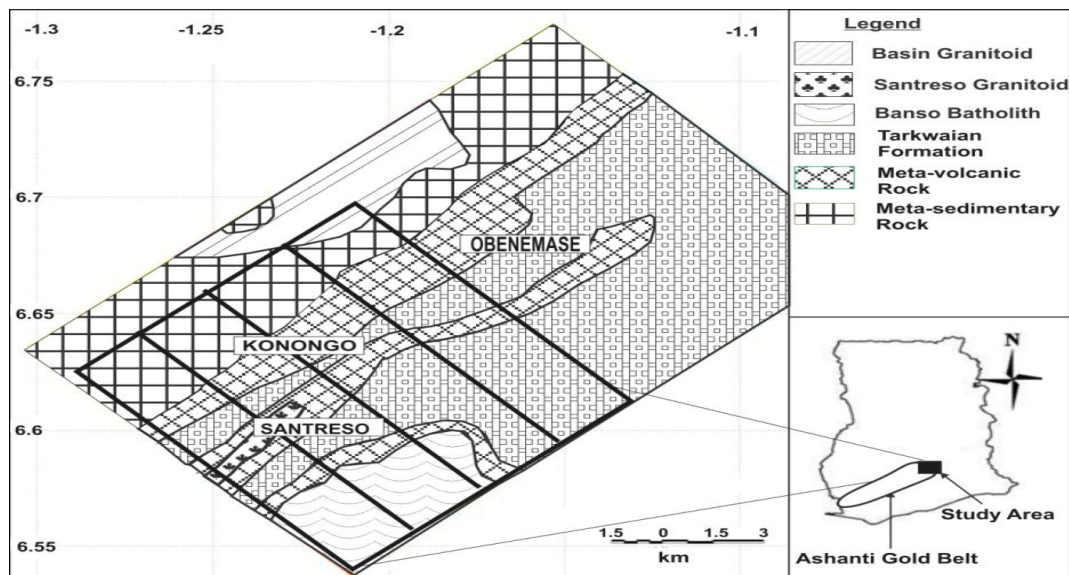


Figure 1. Geological map of the Konongo area (Modified From Griffis et al. (2002))

contacts where chromite mineralization in serpentinite and iron ore in shale had been located (Kesse, 1985). The survey provided magnetic maps showing detailed geological structures of the area. Geotrex (now owned by Fugro Airborne Services) in 1993 used two airborne geophysical survey techniques namely a 125 Hz base-frequency airborne time-domain electromagnetic (GEOTEM) and magnetic over the southernmost portion of the Ashanti Greenstone Belt with an area cover of about $2.7 \times 10^3 \text{ km}^2$ (Asiamah, 2004). Sub-parallel regional shear structures that traverse the study area continuously up to 40 km were delineated as well as a 5 km strike-length, section of the western-most shear zone. According to Telford et al. (1990) the physical principles of aeromagnetic methods are based on taking measurements of the ambient magnetic susceptibility of the surface geology and using the data to determine the distribution of magnetic minerals and hence changes in lithology. Wilford et al. (1997) indicated that airborne radiometric survey similarly is used to measure variations in the radioactive mineral composition in order to map lateral lithological changes. This method involves the measurement of naturally occurring radioactive elements that exist in rock forming minerals and soil profiles. These elements are uranium (U), thorium (Th) and potassium (K), which can be found as trace elements in all rocks and decay naturally giving off gamma radiation (gamma rays). The variation of magnetic and radiometric mineral composition in rocks due to the different in lithological set up and mineralization processes such as hydrothermal mineralization make the use of these methods in the mapping rock lithology, structures and mineral zones an important technique.

This paper discusses aeromagnetic and radiometric datasets from the Konongo area of the Ashanti Gold Belt

of Ghana. This is to help map the geology and to delineate possible gold hosting structure within this part of the belt. The data used in this work was collected in 1997 as part of geophysical data collection programme in Ghana by Geological Survey of Finland (GKT) to support the mining sector in the country and other gold production belts of Ghana. This research seeks to review the geology and to aid the delineation of regional and local geological structures (shear zones and faults) that have the potential of hosting gold mineralization within the study area. The work supplements the effort and allows the prediction of target areas for detailed exploration work in search for metal ore mineralization within the Konongo area that has not been extensively explored as compared to the other parts of the Ashanti Belt.

Geology and Mineralization

Ghana falls mostly within the West African Craton which stabilized in the early Proterozoic (2000 Ma) during the Eburnean Orogeny (Kesse, 1985). The Ghana shield area has two main rocks system, the Birimian with its associated granitoid intrusives and the Tarkwaian Formation. The Birimian was deformed, metamorphosed and intruded by syn- and post-granitoids during the Eburnean orogeny at 2130-1980 Ma, (Feybesse et al., 2006). In elongated basins which follow the north-easterly trending Birimian belts, middle Proterozoic molasse type sediments of the Tarkwaian formation were deposited (Kesse, 1985).

The geology of the area (Figure 1) is dominated by NE trending bands of Birimian meta-sediments/volcanics and the Tarkwaian clastic formation. To the east, the Tarkwaian formation widens out very substantially and to

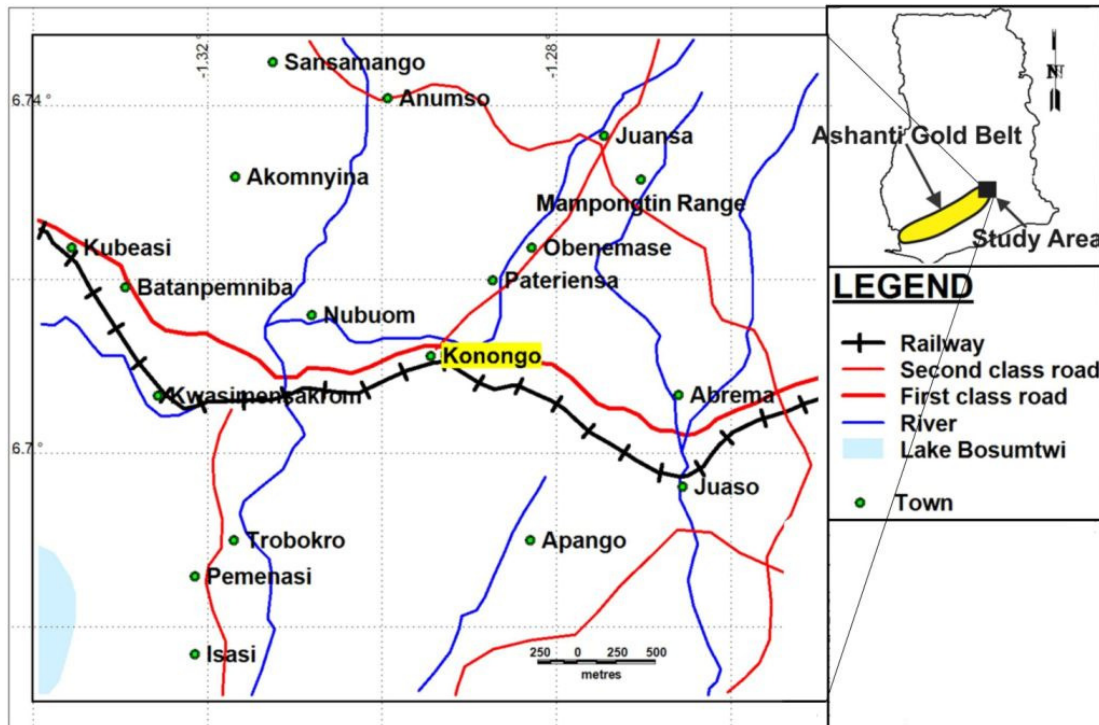


Figure 2. The Konongo Area (Study area)

the west of the district, there are mainly Birimian meta-sedimentary units of the Kumasi Basin. Within the basin domain are large masses of basin-type granitoids belonging to the Kumasi Complex (Griffis et al., 2002). The south-east of the district is dominated by the unusually large Bansa batholith, which is rich in radiometric potassium (Griffs, 1998). Early workers in the area (Hirst, 1942) believed this granitoid to be post-Birimian and pre-Tarkwaian because of the lack of contact metamorphic effects in Tarkwaian formation close to the batholith. However, recent work has challenged this view and it appears that the Bansa batholith is a fairly late-stage intrusion that apparently post-dates the Tarkwaian formation (Griffis et al., 2002).

Gold mineralization is commonly associated with these fault zones and with a complex array of deformed quartz veins and arsenopyrite-silica-sericite-carbonate alteration (Oliver, 2009) which are useful exploration targets (Adjovu, 2006). Structurally the study area covers a segment of the Konongo-Axim Shear System. This shear zone occurs close to the belt margin and hosts a number of deposits and operating mines. The rocks of the area are variable grained, sheared, metamorphosed quartzite containing a constant level of mafic and carbonaceous minerals, presumably derived from syngenetic volcanic activity.

Metamorphic grade of the Birimian rocks is that of the greenschist facies (Adjovu, 2006), with local amphibolite facies aureoles around granitoid plutons. Recent work in the southern Ashanti Region (John et al., 1999) suggests

that the greenschist facies is widely retrograde after amphibolite facies conditions.

MATERIALS AND METHODS

Study site description

The study area is located around Konongo (Figure 2), the capital of the Asante Akim North District. It is 50 km from Kumasi (Ashanti Regional Capital) and about 230 km from Accra, the capital of Ghana. The study area is defined by the pillar coordinates P1, P2, P3, P4 and P5 (see Figure 3A respectively) $(-1.0593^{\circ}, 6.7297^{\circ})$, $(-1.1956^{\circ}, 6.7302^{\circ})$, $(-1.3222^{\circ}, 6.6100^{\circ})$, $(-1.3222^{\circ}, 6.4862^{\circ})$ and $(-1.0584^{\circ}, 6.4866^{\circ})$ projected in the World Geodetic System (WGS) 84.

The topography of Konongo is that of an undulating land. To the north of the District is the prominent Kwahu escarpment, where elevations are about 550-600 m above sea level (ASL) near Agogo. The escarpment stands well above the low rolling hills in much of the District, where elevations are mainly in the range of 180-260 m ASL. In the SE corner of the District is the very large batholith of the Bansa intermediate granitoid with a peak elevation of about 580 m ASL in the central area of the batholith. The annual rainfall of the district averages between 150-170 mm. The daily temperature ranges from 22°C to 30°C with minimum monthly temperature of 26°C and maximum temperature of 30°C recorded in

Table 1. Airborne Geophysical Survey Equipment (Geological Survey of Ghana, 1998)

Survey Equipment	Aircraft (Fixed wing)	Magnetometer	Spectrometer
Equipment Types	Cessna Titan 404 (C-FYAU)	Scintrex Cesium SC-2	Exploranium GR 820-256 with 2048 in ³ NAI (TI) downward looking crystal and 256 in ³ upward looking crystal

Table 2. Airborne Geophysical Survey Parameters (Geological Survey of Ghana, 1998)

Survey Parameter	Parameter Specification
Year	1997-1998
Travel line spacing	400 m
Travel line direction	NW-SE
Tie-line spacing	5000 m
Tie-line direction	NE-SW
Nominal terrain clearance	70 m
Navigation	Global Positioning System (GPS)
Sampling time	0.1 s (magnetic), 1.0 s (radiometric)
Air speed (nominal)	250-290 km/h (70-80 m/s)
Measurement spacing	8 m (magnetic), 80 m (radiometric)

March and April. The average humidity in the area is 75-80 %.

Data acquisition and metadata

The Geological Survey of Finland (GKT) in collaboration with the Geological Survey of Ghana and the Ghana Minerals Commission in the years 1997-98 carried out systematic airborne geophysical survey in southern Ghana, which the Ashanti belt was part. The survey produced high resolution airborne geophysical information for geological mapping and mineral exploration purposes. Among the airborne geophysical datasets collected include magnetic, radiometric and electromagnetic datasets.

The data was collected with the following aircraft equipment (Table 1) and survey parameters (Table 2).

Data processing

The major software used to process and enhance the data is the Geosoft (Oasis Montaj). Other geophysical software that were used to enhance the data in a variety of formats are, Golden Software Surfer 10, Model Vision Professional 8 and MapInfo - Discover 11.1. The processing of airborne data involved the sequential processes of editing, the application of a gridding routine, and removal of the Earth's background magnetic field.

Some corrections like removal of diurnal variation of the Earth's magnetic field, aircraft heading, instrument variation, lag error between aircraft and the sensor and inconsistencies between flight lines and tie lines were made by the Geological survey of Finland (GKT). The geophysical data set from the Konongo project area were co-registered to Longitude-Latitude Coordinate System.

Extraction of the raw data from original tapes and locating the data in x and y coordinates with Geosoft software constituted the pre-processing phase. The main processing phase comprised of four steps: gridding, calculating the definitive geomagnetic reference field (DGRF) to be subtracted from the observed magnetic data, micro-leveling the entire data set to remove any apparent residual errors, and merging the different blocks for each different data type.

Aeromagnetic data

The *magmap* tool (Oasismontaj, Geosoft) offering a number of utilities was implemented to help calculate the magnetic-anomaly grid (total field intensity minus the Definitive International Geomagnetic Reference Field) for the appropriate time of year. After producing the grid the necessary filters were applied to it before displaying the image with the *Grid and Image* tool.

A range of imaging routines were applied to visually enhance the effects of selected geologic sources using mathematical enhancement techniques (Milligan and

(Gunn, 1997). In order to facilitate interpretation, Analytic Signal Amplitude and Two-Dimensional Fast Fourier Transformation (2D-FFT) filters were applied to enhance the quality of the magnetic data. The 2D-FFT filters used included Reduction to Pole, First Vertical Derivative and Upward Continuation Derivative.

Aeroradiometric data

The *Grid and Image* tool was used to create the total count images after micro-leveling the entire data set to remove any apparent residual errors. The images were then correlated with the pattern and trend of the geological units for geochemical mapping of the radioactive elements potassium (K), uranium (U) and thorium (Th).

In order to recognize and understand radiometric signatures associated with the host rocks important to mineralization, enhancing techniques such as composite image, ratio maps as well as potassium (%K), equivalent thorium (eTh ppm) and equivalent uranium (eU ppm) maps were used. These were to help identify zones that have high concentrations of potassium and thorium which is generally considered very immobile. This is because of the role they play in the delineation of gold mineralized zones since gold deposits show increases in K and Th, which suggest that Th was mobilized in hydrothermally altered systems (Silva et al., 2003).

RESULTS AND DISCUSSION

Airborne magnetic and radiometric datasets were used to delineate the geology, structure and alteration zones in the study area. The airborne radiometric and magnetic data generated high resolution maps that show major lithology and structural features present in the Konongo area. The purpose of the interpretation of these maps is to identify the individual lithology and delineate geological structures which control gold mineralization in the area. Elevated radiometric element patterns and low magnetic susceptible areas which might have resulted from rock alterations or possible mineral deposits are delineated as potential targets for ore deposits.

Interpretation of magnetic data

Magnetic anomalies in the Earth's magnetic field are caused by magnetic minerals in the rocks, and maps of these anomalies can be interpreted in terms of geology (Silva et al., 2003). The main goal for the use of the magnetic data is to delineate geology and structures which normally serve as conduits for hydrothermal fluid deposition. The concentration of magnetic minerals or their excessive destruction by hydrothermal alteration especially along tectonic structures enhances the use of

this method for the detection of geological structures (Plumlee et al., 1992).

Figure 3A shows different magnetic anomalies corresponding to different lithology and geological structures in the study area. Due to the location of the study area (point of low magnetic latitude) the total field magnetic map shows high magnetic susceptible areas in low magnetic values and vice versa. The polygons in Figure 3B (contour of TMI map) indicate areas that are tectonically disturbed.

The long stretch low magnetic susceptible pattern M_S , corresponds with the meta-sedimentary rock (Argillite and Siltstone) (Figure 3A). A dome shaped-granitoid structure is reflected at the bottom and this corresponds to the Banso Batholith (BB). The broad NE-SW high magnetic susceptible patterns M_{V1} , M_{V2} and M_{V3} at the central-part of Figure 3A, represent the meta-volcanic rocks (volcaniclastics) separated by the Tarkwaian Formation (T_F). The contour map (Figure 3B) indicates that M_{V1} , M_{V2} and M_{V3} which were NE-SW striking continuous geological units have been folded, fractured and faulted by the different tectonic regimes producing a splay of faults, thus introducing a structural corridor (area of the blue polygon) at the northwest of the Banso Batholith. The folding of T_F , M_{V1} and M_{V2} at the central part of the area may be attributed to the intrusion of Banso Batholith (Figure 3B) and the discontinuity of M_{V1} at the north of the BB is as a result of shearing and faulting (Figure 3A). In Figure 3B the meta-volcanics north-west of the Banso Batholith is more tectonically disturbed (faulted, fractured and sheared by the intruding dolerite dike system) increasing rock permeability thus has the potential to host hydrothermal fluids.

In order to locate the observed magnetic anomalies directly over the magnetic source bodies, the TMI grid was transformed into reduction to the pole (RTP) grid map (Murphy, 2007) using the 2D-FFT filter. This map of RTP (Figure 3C) sharpens the contacts between the magnetic high and low patterns as well as anomalously high magnetic susceptible zones probably coming from deeper sources. The structures S_1 - S_1 and F_N - F_N representing faults were not clearly noticed in the TMI grid but were well exposed in the RTP grid.

The low magnetic anomaly around the batholith (BB) in Figure 3C is as a result of contact metamorphism. Analytical maps are useful as a type of reduction to pole when applied to magnetic data collected from low magnetic latitude such as the study area. The analytic signal amplitude is independent of the direction of the magnetization of the source and is related to the amplitude of magnetization (Nabighian, 1972; Roest and Pilkington, 1993). This technique as applied to the TMI data in Figure 3D helped to clearly display the edge extent and contacts between the different formations in the area. Three high anomalous zones (M_{V1} , M_{V2} and M_{V3}) trending in the NE-SW direction which are associated with the meta-volcanics unit are observed in

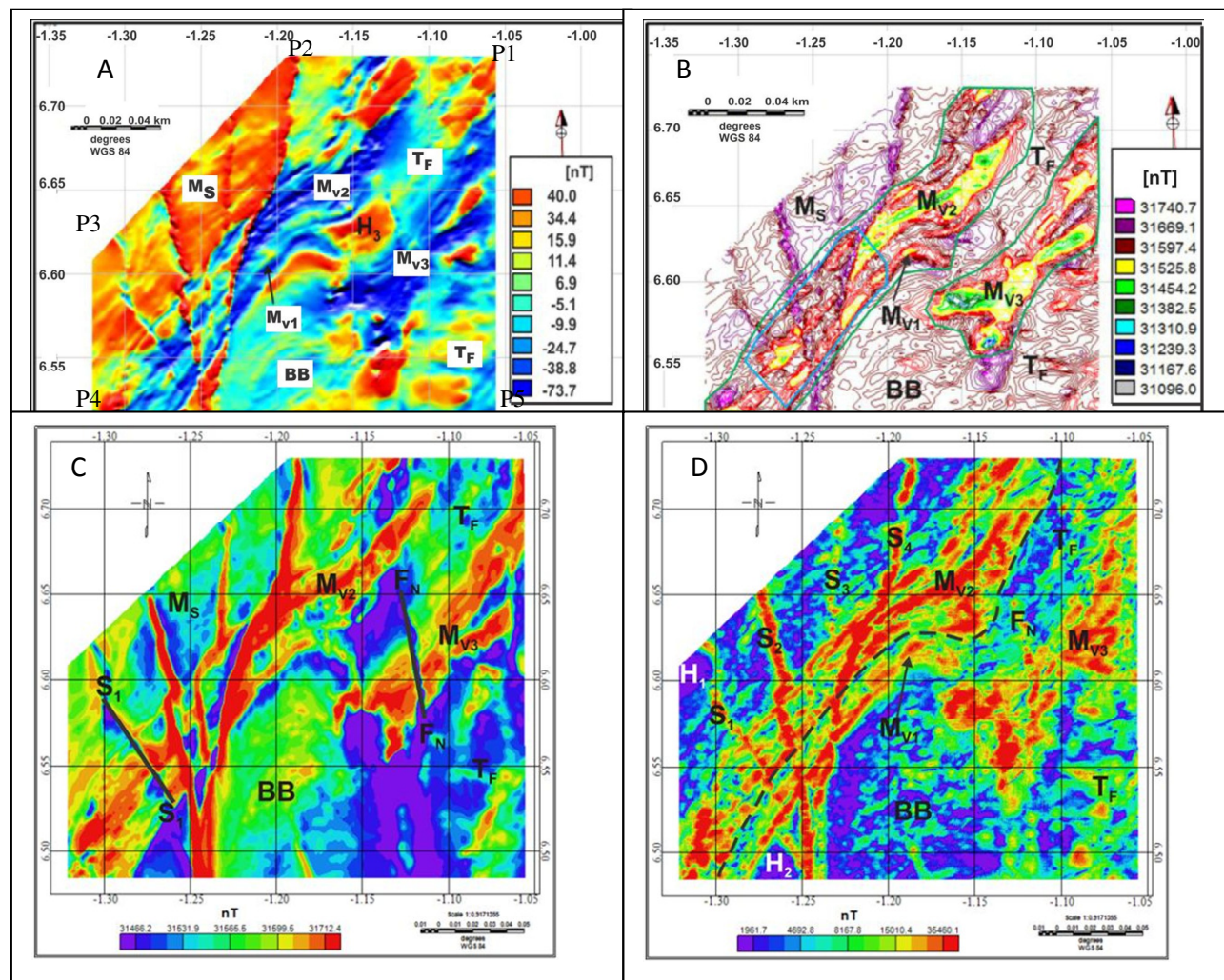


Figure 3. (A) Residual total magnetic intensity (TMI) grid map, (B) Contour map of TMI, (C) TMI grid ($I = -12.34^\circ$, $D = -5.73^\circ$) reduced to pole, (D) - Map showing the analytical signal amplitude.

this image. H_2 is part of the Bansa Batholith that has been cut off by the dolerite dike system. The features S_2 , S_3 and S_4 with high magnetic anomalies (Figure 3D) are intrusions (dikes) that traverse the Birimian system and batholith in the region. Another linear feature F_N in the N-S direction cuts across the M_{V3} and the Tarkwaian formation (T_F).

Figure 4A is a first vertical derivative (1VD) image displaced in gray scale. The 1VD operator helped to attenuate broad, more regional anomalies and enhance local, more subtle magnetic responses because of their sensitive to shallow magnetic source bodies and contacts (Gunn, 1975; Keaty, 1995). The magnetic map (Figure 4B) which is tilt derivative of the TMI map (Figure 3A) also helped to deduce the subtle geological boundaries of the various structures enhanced by the other filtered grids.

The elongated folded meta-volcanic unit M_{V2} seen in the TMI (Figure 3A) and RTP (Figure 3C) maps is rather better exposed in the 1VD map (Figure 4A) as a

collection of faulted structures trending in the NE-SW direction with the boundary well defined. The dike S_5 is noted to intrude the Bansa Batholith and fault F_M marks the contact between batholith and the Tarkwaian Formation. S_2 , S_3 and S_4 of the N-S trending, late-stage dolerite dike system (Figure 4A) at the contact zone of M_S and M_{V2} is shifted to the NE direction resulting from late activation of the D_1 deformations thus resulting in hanging wall and foot wall in the meta-sediments and meta volcanics respectively.

Figure 4C is a representation of the delineated geological structures superimposed on the RTP map (Figure 3C). This map (Figure 4C) gives an idea about the depositional time-sequence of formation of the lithological units and some geological structures in the Konongo area. At the upper right corner of Figure 4C, F_N which was once a continuous structure has been traverse by M_{V2} creating F_{N1} . Also S_1 , S_2 , S_3 and S_4 are seen to traverse across M_{V1} , M_{V2} and BB while F_N traverses across M_{V3} and the Tarkwaian Formation. Thus it can be

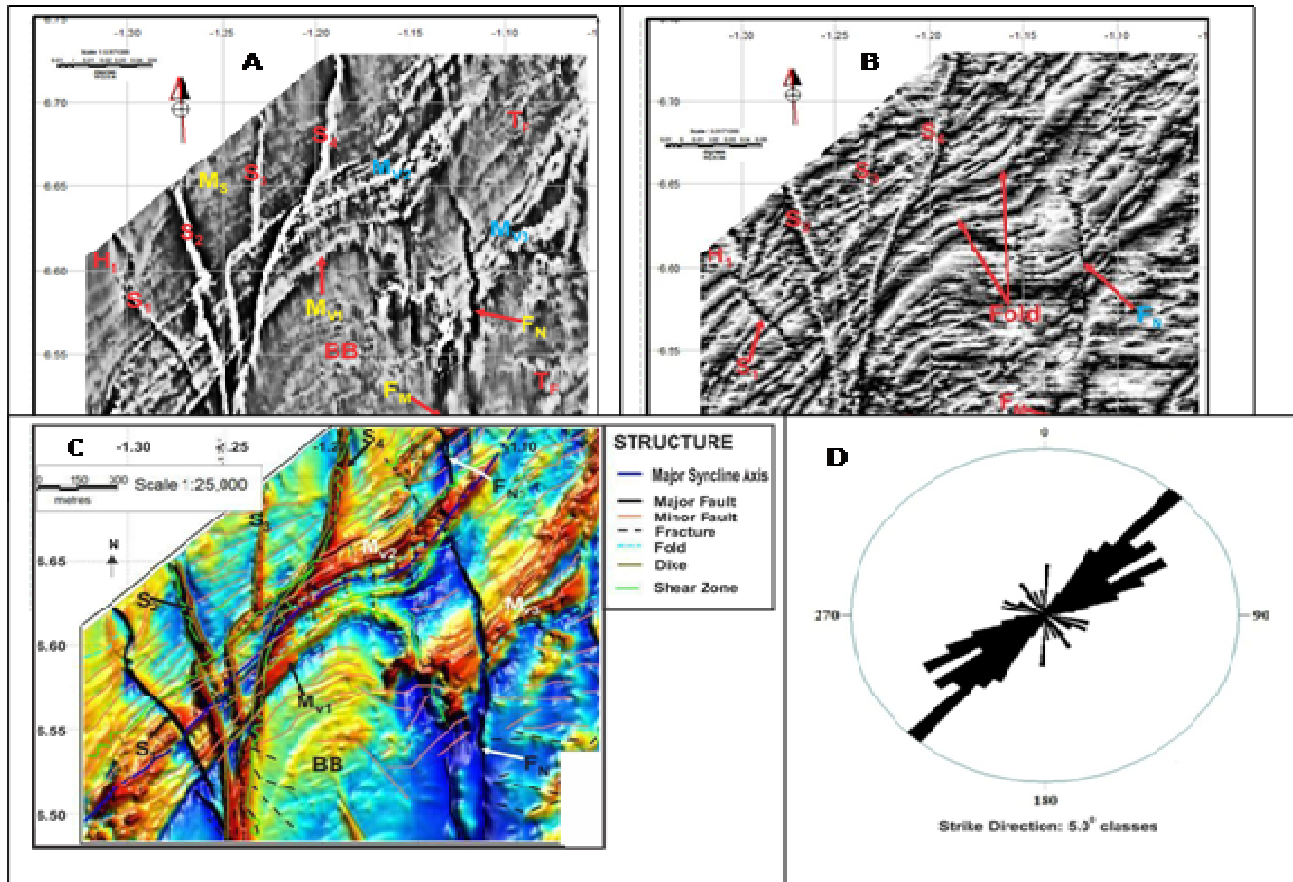


Figure 4. (A) First order vertical derivative map. (B) magnetic TDR map in gray scale. (C) Interpreted geological structure map superimposed on the RTP map. (D) Equal area rose diagram

inferred that M_3 is the oldest among the meta-volcanic rocks while M_3 , M_1 and BB are younger than F_N but older than S_1 , S_2 , S_3 and S_4 . The folding and shearing of M_{V1} and M_{V3} respectively by the Bansa Batholith suggests that the Bansa Batholith is the youngest among the lithological units. The interpreted magnetic structural map reveals enhanced structural features that include shear zones, faults, shear and fault intersections and fracture systems as magnetic anomalies that mainly trend NE-SW. The structural features throughout southwestern Ghana are believed to have resulted from one major, progressive NW-SE deformational event (Eisenlohr and Hirdes, 1992) which is thus responsible for the folding of the discontinuous structures of M_{V2} and M_{V3} . The area (Figure 4A) also features a major, N-S trending, late-stage dolerite dike system that cuts across the Bansa Batholith and splits up into at least three (3) structures in the meta-sediments. Faults that evolved through linkage are commonly associated with sets of splays that break off the main faults. Each splay accommodates a portion of the deformation transferred from the main faults and has its own termination point (Murphy, 2007). This is quite obvious where there are a large number of magnetic

markers striking perpendicular to the structures S_1 , S_2 , S_3 , S_4 , F_M and F_N (Figure 4B).

Figure 4D shows an equal area projection rose diagram (azimuth-frequency) for lineaments delineated from aeromagnetic maps showing frequency of observed faults strike direction, in 5° classes. Lineaments delineated on the imagery depict trends in the NE-SW, NNE-SSW, E-W, NNW-SSE and N-S directions. The rose petals in the NE-SW and NNE-SSW represent the main strike directions in the Birimian formation. The Figure 4D indicates that out of 120 azimuths values plotted 12% represented the largest petal which strikes 40° - 50° (NE-SW) which corresponds to the D_1 structures. About 60% of the total azimuth values range between 30° and 70° (NE and NNE) strike which represents the regional strike of the lineaments (Griffis et al., 2002) and corresponding to the D_1 and D_2 structures. A little over 8% of the azimuths have values approximately at 40° and almost 20% have strike values between 100° and 180° (NW-SE).

Interpretation of radiometric data

A number of potassium anomalies are evident in the

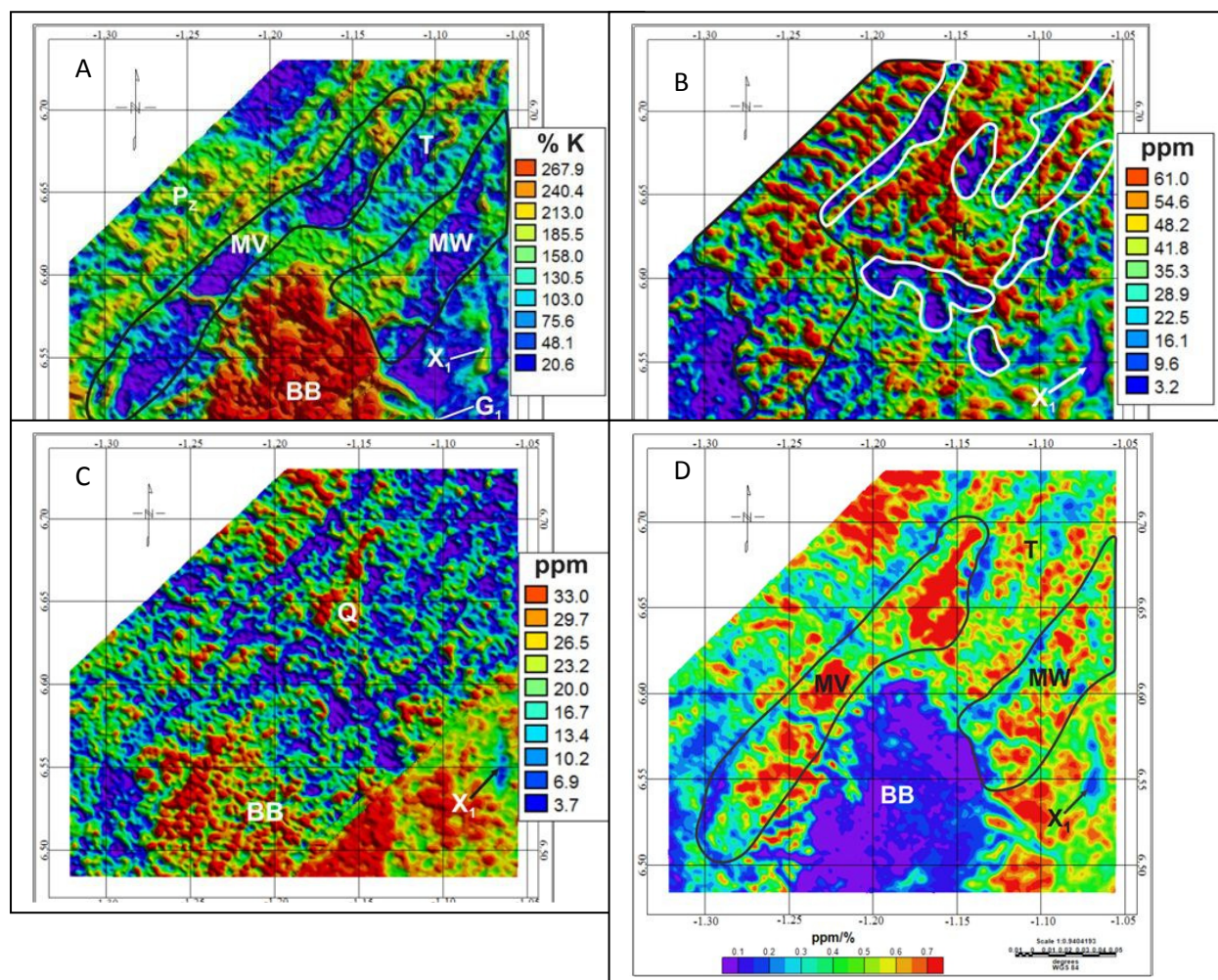


Figure 5. Gamma spectrometric image for: **A** - potassium (K) concentration, **B** - thorium (eTh) concentration, **C** – uranium (eU) concentration and **D** – ratio of eTh/K

radiometric survey image Figure 5A. A particular strong anomaly occurs in the central-south and this coincides with the Bansa (batholiths (BB)) which Griffis et al. (2002) described to be an intrusive high K granitoid. Potassium radiation essentially comes from K feldspar, predominantly microcline and orthoclase or micas such as muscovite and biotite which are common in felsic igneous rocks (e.g. granite) and are low in mafic rocks (e.g. basalts and andesite) but virtually absent from dunite and peridotites (Manu, 1993). Comparing Figure 5A to the TMI map (Figure 3A) the elongated high radiometric anomalous zone P_z , hosting K concentrations linearly distributed in the NE-SW direction represent the coarse grained meta-sediment unit M_s . The Meta-volcanic units M_{V2} and M_{V3} have low K concentration (MV and MW) but M_{V1} and the Tarkwaian formation (noted as T in Figure 5A) have moderate K concentration. High Th concentrations are related to felsic minerals and low Th concentrations are related to mafic minerals (Shives, 2008). The Bansa granitoid registered moderate Th concentration (Figure 5B). The strong thorium

concentration in the region marked by the black polygon is as result of highly weathered colluvial deposits into the lowlands. Thorium is generally considered very immobile (Silva et al., 2003) thus the regions with low thorium concentration suggest Th was mobilized in hydrothermally altered systems. The low Th patterns (white thick polygons in Th image Figure 5B) represent alteration patterns in the different rocks and along lithologic boundaries. Along these regions are also faults and shears (Figure 4B) hosting hydrothermal fluid which leach Th concentration.

Unlike the K and the Th maps, the U map (Figure 5C) could not clearly indicate distinct boundary between the meta-sediment and meta-volcanics. The areas marked by white polygons in Figure 7B also recorded low U concentration. The high U concentration is at the south and south-east of the area with the feature X1 which recorded high K and low Th, recording high U. Histogram stretching and band rationing of the channels were used to maximize contrast and highlight subtle features in the data. The Th channel and ratio map of Th/K were used to

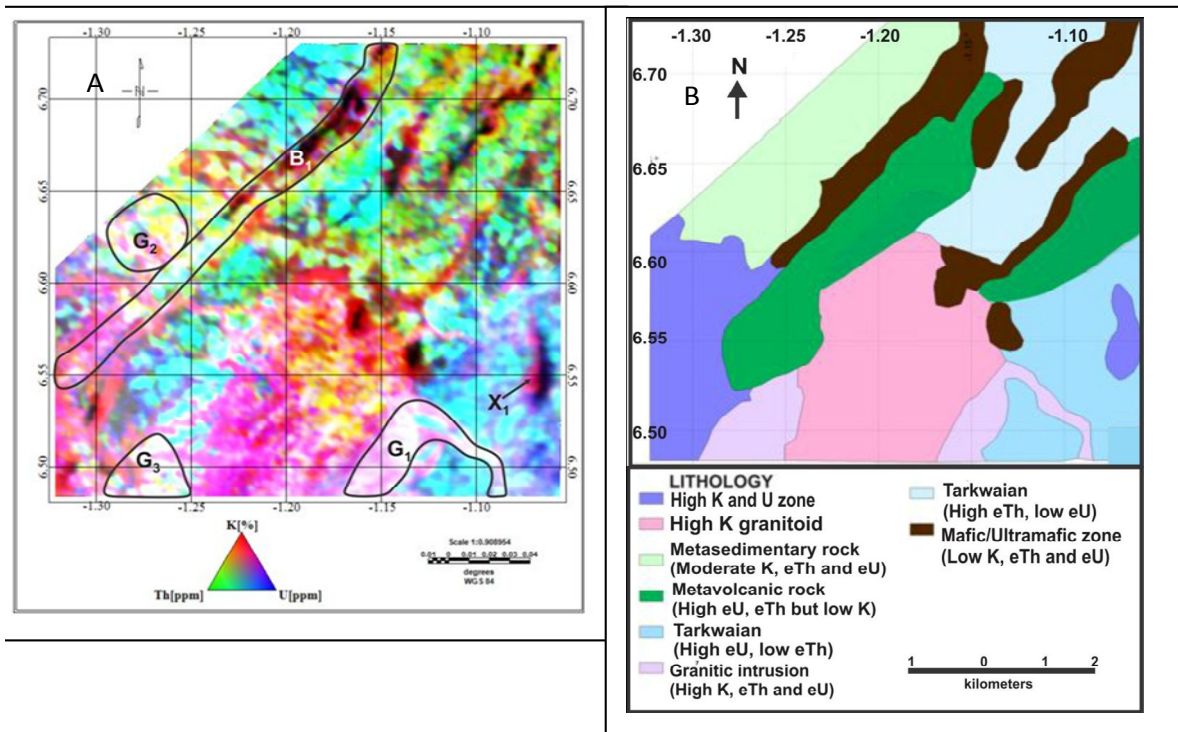


Figure 6.A - Ternary Image (RGB=KThU) of the Study Area. **B** - Preliminary interpreted geology from airborne radiometric data

assess the degree to which the source materials of regolith are weathered or leached since K response is associated with easily weathered minerals, whereas Th and U are typically associated with residual clay, oxides and accessory minerals (Wilford et al., 1997). Figure 5D represents thorium-potassium ratio (Th/K) concentrations which map some lithologic contrast and enhanced alteration signatures. The increase in K content and decrease in Th/K ratio observed for the mafic meta-volcanic rocks (MV and MW) is indicative of hydrothermal alterations. This is because mafic volcanic rocks generally lack K-bearing minerals and K enrichments are not accompanied by Th during hydrothermal alteration processes (Dickson and Scott, 1997). Generally, K and other metal constituents are added to the host rock by hydrothermal solutions, and it is easily observed in mafic units or along lithologic contacts where hydrothermal alteration such as silicification is intensive.

The Ternary image Figure 6A comprises of colours generated from the relative intensities of the three components and represents subtle variations in the ratios of the three bands. Potassium was assigned to red, uranium to blue and thorium to green. The magnetite and quartz-rich sandy materials appear darker than the surrounding units, indicating lower concentrations in K, U, and Th. The white areas in the ternary image are indication of high concentration of potassium, thorium and uranium resulting from felsic volcanic materials. The magenta shows areas of high K and U but low Th concentrations whilst the yellow indicates areas of high K

and Th but low U concentrations. The ternary map shows high thorium concentration in the north-east while the Bansa Batholith and the south-western corner of the image record high K. The X₁ formation has its boundary delineated and the constituent radiometric elements are K and U.

The most significant radiometric response in both the potassium and uranium maps (Figures 5A and 5C) recording high concentration of K and U respectively is associated with the Bansa granitoid within the region. The Tarkwaian formation was identified by the significant Th signature at the north-east and south-east of Figures 5D and 6A. The meta-volcanic rocks (M_{V1}, M_{V2} and M_{V3} in Figure 3A) have high magnetic anomalies, but possess very low K and Th concentrations and the K normalized map of Figure 5A (low K concentration) showed their distinct boundaries. The meta-sedimentary unit M_S did not show unique radiometric signature however, displayed distinct radiometric boundaries that correspond much well with magnetized lineaments, (Figure 5A). The low Th patterns (white thick polygons in Th image, Figure 5B) between the Tarkwaian formation, meta-volcanics, granitoid and meta-sediment correspond with the alteration patterns along lithologic boundaries and with the Tarkwaian formation. The areas which reflect mobilization of immobile Th concentration also indicated hydrothermally altered zones.

Silva et al. (2003) made some remarks, indicating that radiometric data are an excellent tool which helped in mapping and tracing of individual lithological units in

Areas of outcrop. The mafic, ultramafic and paleoproterozoic units are distinctive in potassium and ternary maps (K, Th and U) because of their low radiometric signature (Figure 6A). The granites and dacitic rocks have a high total count radiometric response, appearing as white or blue (high uranium) in the ternary image (Figure 6A).

CONCLUSION

The principal geological structures hosting many of the epithermal and mesothermal gold deposits include faults, fractures and shear zones play the most important role in gold mineralization in the Birimian of Ghana (Allibone et al., 2002). The continuous reactivation of these structures has had profound effect on both the distribution and the mode of gold mineralization throughout the country (Cozens, 1989). Therefore delineated structures of the study area are likely to be potential hosts of metal ore mineralization. From the interpreted composite structural map (Figure 7) three episodes of deformation D_1 -NE, D_2 -NNW and D_3 -NNE were observed. The early deformational event D_1 produced sets of NE-SW striking local and regional faults and fractures. D_2 deformational event produced mainly NNW-SSE and NW-SE faults and fractures some of which intersected the earlier D_1 structures. At the northern and the eastern parts of the study area D_1/D_2 intersections are observed. The D_3 event produced NNE-SSW set of faults and fractures produced by splay of dikes (S_2 , S_3 , and S_4) which are more associated with the Bansa Batholith, and reactivated some D_1 and D_2 faults and fractures which are observed in the locality of S_5 .

Structures in the area are certainly complex and feature tightly folded and faulted bands of Birimian series and Tarkwaian formation; the trends of the major faults as well as the fold planes, strike to the NE and dip steeply to the NW. The area also features a major, N-S trending, late-stage dolerite dike system (Griffis et al., 2002) that cuts across the Bansa Batholith (creating H_2 in Figures 4A and 4B) and splits up into at least three branches noted as S_2 , S_3 and S_4 that extend through the area.

The area is dominated by a series of NE trending shears (green lines in Figure 7A) which are interpreted as high angle fault structures formed during regional NW-SE compression. A higher degree of shearing and faulting at the contact zone of the meta-sedimentary and meta-volcanic have caused shifting of the dikes S_2 , S_3 and S_4 towards NE direction thus creating hanging wall and foot wall in the meta-sedimentary and meta-volcanic rocks respectively (Figure 4A).

The altered region marked X_2 (Figure 6A) which is associated with the Bansa Batholith has high potassium and thorium concentration. The regions A1, A2, A3 and A4 in Figure 7B recorded low magnetic anomalies

(Figures 3C and 3D) due to the increase in rock permeability (intense faulting and shearing thus the ability to host hydrothermal fluids). These regions also recorded high K but low Th and U concentration thus qualifying for hydrothermally altered zones. Graphite, mica, and euhedral to anhedral disseminated Fe sulphides observed in the host rocks in the study area (Cozens, 1989) are interpreted to be hydrothermal alteration products, potentially related to gold mineralization. Evidence of alteration that preceded gold mineralization is best preserved in spatially associated altered mafic dikes S_2 , S_3 , and S_4 (Figure 3D). The magnetic survey identified high magnetic contrast between rock bodies along the contact zone, interpreted as a potential pathway for fluid migration and mineralization. The dike system (S_2 , S_3 and S_4) and the fault S_1 cut across NE trending D_1 structures (Figure 7A) thus rendering these contact zones more permeable and fractured for accumulation of hydrothermal fluids. The sheared zone that trends NE-SW along the S_4 dike is of much importance. It cuts across the contact zone of the geological unit and the regional synclinal axis as well as D_1 structures along its path.

In order to predict favourable locations for possible blind ore deposits in the study area, both structural and alteration patterns were taken into consideration. High structural connectivity and areas of intensive alterations reflected as low magnetic anomalous and high K concentration were considered particularly, where the two alteration types coincide and also marked by faults, fault intersections, fractures and shear zones. The features marked A1, A2, A3 and A4 (Figure 7B) are areas with high potential for gold mineralization with A1 and A2 bearing the most potential. The regions G_1 , G_2 and G_3 (Figures 6A and 7B) mark areas with high K, Th and U concentration. High K and Th concentration but low U is mark by X_1 . The hydrothermal alteration zone A3 that marked the contact between the Meta-volcanic and the Tarkwaian Formation can also be considered as potential target. An integrated geological map from radiometric and magnetic datasets established links between lithology, structures and hydrothermal alteration patterns. The relationship shows that the hydrothermal system is structurally controlled and not limited to any specific lithology or host rock. Moreover, the area is also marked by quartz veins, concordant with the potential mineralized zones allocated along the contact of the Meta-volcanic and Tarkwaian formation, indicating the region of higher fluid pressure and accumulation of silicate minerals.

The application of integrated airborne geophysical data (magnetic and radiometric) in the study area to predict zones which have the ability to host mineralization have shown that the technique is potent and could be applied in deeply weathered terrains or regolith regions to pick exploration targets for blind ore deposits. The mapped geological structures, lithology and other hydrothermally altered zones (playing the role of

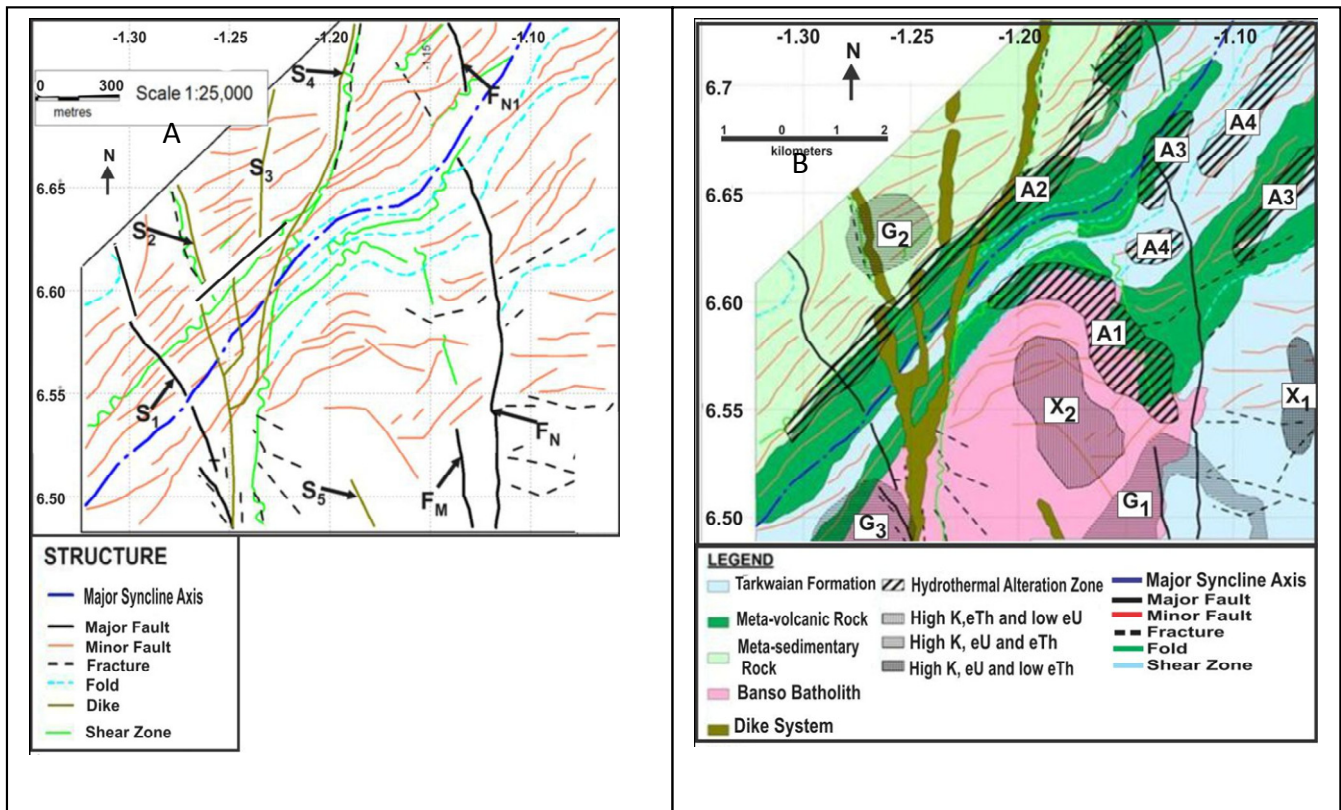


Figure 7. (A) Interpreted structural map from the aeromagnetic datasets. **(B)** Proposed geological and structural map of Konongo area

mineralization indicators) from the aeromagnetic and radiometric datasets have added to the proposal of many authors such as Cozens (1989) and Griffis et al. (2002) regarding the Konongo area as potential host of commercial gold deposits.

ACKNOWLEDGMENTS

We are most grateful to Ghana Geological Survey Department (GGSD) for giving access to their aeromagnetic and aeroradiometric data for this work and Newmont Ghana Gold Limited (NGGL) for providing the software for the data processing.

REFERENCES

- Adjovu I (2006). Nyinahin Concession. *Technical report-Mikite Gold Resources Limited*.
- Airo M L, Karell F (2001). Interpretation of airborne magnetic and gamma-ray spectrometric data related to Mammashti Cu-Zn-Au deposit in eastern Finland. *Special Paper*, 31: 97–103.
- Airo M L, Loukola-Ruskeeniemi K (2004). Characterization of sulfide deposits by airborne magnetic and gamma-ray responses in eastern Finland. *Ore Geology Reviews*, 24 (1):67-84.
- Allibone A, Teasdale J, Cameron G, Etheridge M, Uttley P, Soboh A (2002). Timing and structural controls on gold mineralization at the Bogoso gold mine, Ghana, West Africa. *Economic Geology*, 97(5):949–969.
- Armstrong M, Rodeghiero A (2006). Airborne Geophysical Techniques in Aziz. *Coal Operators' Conference* (pp. 113-131). University of Wollongong and the Australasian Institute Mining and Metallurgy.
- Asiamah GK (2004). The South Ashanti Greenstone Belt GEOTEM And Magnetic Survey- Application to Mineral Exploration. *2004 SEG Annual Meeting*. Denver, Colorado: Society of Exploration Geophysicists.
- Cozens B (1989). The geology and structure of the Konongo gold mine, Ghana, and its implications in exploration. In Le Maitre R. W. (ed.) *Pathways in geology- essays in honour of Edwin Sharbon Hills.*, (Pp. 439–456). Blackwell, Melbourne.
- Dickson BL, Scott KM (1997). Interpretation of aerial gamma ray surveys-adding the geochemical factors. *AGSO Journal of Australian Geology and Geophysics*, 17 (2):187- 200.
- Eisenlohr BN, Hirdes W (1992). The structural development of early Proterozoic Birimian and Tarkwaian rocks in southwest Ghana, West Africa. *J. Afri. Earth Sci.*, 14 (3):313–325.
- Etheridge M, Rutland R, Wyborn L (1987). Orogenesis and tectonic process in the early to middle proterozoic of northern Australia. *Proterozoic lithospheric evolution*, 17 :131-147.
- Feybesse JL, Billa M, Guerrot C, Duguey E, Lescuye JL, Milési JP (2006). The Paleopro-terozoic Ghanaian Province: Geodynamic Model and Ore Controls, Including Regional Stress Modelling. *Pre-cambrian Res.*:149(3-4):149-196.
- Griffis RJ (1998). Explanatory Notes - Geological interpretation of geophysical data from Southwestern Ghana. Minerals Commission.
- Griffis RJ, Barning K, Agezo FL, Akosah FK (2002). *Gold deposits of Ghana*. Minerals Commission Report.

- Gunn PJ (1975). Linear transformations of gravity and magnetic fields. *Geophysical Prospecting*, 23:300–312.
- Hirst T (1942). The geology of the Konongo goldfield and surrounding country. *Gold Coast Geological Survey Bulletin*, 14. Implications in exploration. In Le Maitre R. W. (ed.) *Pathways in geology- essays in honour of Edwin Sharbon Hills*: 439–456; Blackwell, Melbourne.
- John T, Reiner K, Geoffrey L, Wolfgang H (1999). The metamorphic evolution of the Paleoproterozoic (Birimian) volcanic Ashanti belt (Ghana, West Africa). *Precambrian Research*, 98:1-2.
- Keating PB (1995). A simple technique to identify magnetic anomalies due to kimberlite pipes. *Exploration and Mining Geology*, 4(2):121-125.
- Kesse GO (1985). *The Mineral and Rock Resources of Ghana*. A.A. Balkema, Rotterdam.
- Manu J (1993). Gold deposits of Birimian greenstone belts in Ghana: Hydrothermal alteration and thermodynamics. Verlag Mainz, Wissenschaftsverlag, Aachen Herstellung: Fotodruck Mainz GmbH Susterfeldstr. 83. 52072 Aachen.
- Milligan PR, Gunn PJ (1997). Enhancement and presentation of airborne geophysical. *AGSO J. Austr. Geol. Geophys.*; 17(2):64-74.
- Milligan PR, Gunn PJ (1997). Enhancement and presentation of airborne geophysical data. *AGSO J. Austr. Geol. Geophys.*; 17(2):64-774.
- Minty, B. R. (1996). The fundamentals of airborne gamma-ray spectrometry. *AGSO J. Austr. Geol. Geophys.*; 17(2):39–50.
- Moon PA, Mason D (n.d.). The geology of Field Sheets 129 and 131, Bompata S.W and N.W. *Geological Survey Bulletin*, 31.
- Murphy BS (2007). Airborne geophysics and the Indian scenario. *J. Ind. Geophysics Union*, 11 (1), 1-28.
- Nabighian MN (1972). The analytical signal of two-dimensional magnetic bodies with polygonal cross-section: its properties and use for automated anomaly interpretation *Geophysics*, 37(3):507–517.
- Oliver B (2009). Million Ounce Gold Project Optioned. Signature Metals Limited, Level 1/33 Richardson Street, West Perth-Australia.
- Plumlee G, Smith KS, Ficklin W, Briggs PH (1992). Geological and geochemical controls on the composition of mine drainages and natural drainages in mineralized areas. *Proceedings, 7th International Water-Rock Interaction Conference*; 419–422. Park City, Utah.
- Reidy P (2012). Konongo Gold Project - Ghana. Auralia Mining Consulting.
- Roest WR, Pilkington M (1993). Identifying remanent magnetization effects in magnetic data. *Geophysics*, 58:653–659.
- Silva AM, Pires AC, McCafferty A, Moraes R, Xia H (2003). Application of airborne geophysical data to mineral exploration in the uneven exposed terrains of the Rio Das Velhas greenstone belt. *Revista Brasileira de Geociências*, 33(2):17-28.
- Telford WM, Geldart LP, Sheriff RE (1990). *Applied Geophysics* (2nd Edition ed.). Cambridge University Press.
- Wilford JR, Bierwirth PN, Craig MA (1997). Application of airborne gamma-ray spectrometry in soil/regolith mapping and applied geomorphology. *AGSO J. Austr. Geol. Geophys.*; 17(2):201–216.